



UNIVERSITY OF LEEDS

This is a repository copy of *Quantification of growth and differentiation of C2C12 skeletal muscle cells on PSS–PAH-based polyelectrolyte layer-by-layer nanofilms*.

White Rose Research Online URL for this paper:

<https://eprints.whiterose.ac.uk/104499/>

Version: Accepted Version

Article:

Ricotti, L, Taccola, S, Bernardeschi, I et al. (3 more authors) (2011) Quantification of growth and differentiation of C2C12 skeletal muscle cells on PSS–PAH-based polyelectrolyte layer-by-layer nanofilms. *Biomedical Materials*, 6 (3). 031001. ISSN 1748-6041

<https://doi.org/10.1088/1748-6041/6/3/031001>

© 2011 IOP Publishing Ltd. This is an author-created, un-copied version of an article published in *Biomedical Materials*. IOP Publishing Ltd is not responsible for any errors or omissions in this version of the manuscript or any version derived from it. The Version of Record is available online at <https://doi.org/10.1088/1748-6041/6/3/031001>

Reuse

Items deposited in White Rose Research Online are protected by copyright, with all rights reserved unless indicated otherwise. They may be downloaded and/or printed for private study, or other acts as permitted by national copyright laws. The publisher or other rights holders may allow further reproduction and re-use of the full text version. This is indicated by the licence information on the White Rose Research Online record for the item.

Takedown

If you consider content in White Rose Research Online to be in breach of UK law, please notify us by emailing eprints@whiterose.ac.uk including the URL of the record and the reason for the withdrawal request.



eprints@whiterose.ac.uk
<https://eprints.whiterose.ac.uk/>

COMMUNICATION

Quantification of growth and differentiation of C2C12 skeletal muscle cells on PSS-PAH-based polyelectrolyte layer-by-layer nanofilms

Leonardo Ricotti^{1,2,3}, Silvia Taccola^{1,2}, Irene Bernardeschi^{1,2}, Virginia Pensabene², Paolo Dario^{1,2}, and Arianna Menciassi^{1,2}

¹ CRIM Lab, Polo Sant'Anna Valdera, Scuola Superiore Sant'Anna, Viale Rinaldo Piaggio 34 – 56025 Pontedera (Pisa), Italy

² Center for MicroBioRobotics IIT@SSSA, Istituto Italiano di Tecnologia (IIT), Viale Rinaldo Piaggio 34 - 56025 Pontedera (Pisa), Italy

Email: l.ricotti@sssup.it

Abstract

Polyelectrolyte layer-by-layer (LbL) nanofilms are interesting polymeric structures, built by alternating adsorption of positively and negatively charged polyelectrolytes. They consist of multilayer sheets with nanometric overall thickness, and they can be used as supports and surface coatings for *in vitro* and *in vivo* cells and tissues growth and regeneration. The present study focuses on nanofilms based on alternated layers of poly(sodium-4-sulfonate) (PSS) and poly(allylamine hydrochloride) (PAH) fabricated using Spin Assisted LbL assembly (SA-LbL). The fabrication process used to assemble polyelectrolyte nanofilms made of up to 60 bilayers is described, and the influence of different surface charges (i.e. changing the terminal layer) and of different film composition (e.g. varying PSS molecular weight) on cell behaviour is investigated. In particular, C2C12 skeletal muscle cells viability, proliferation and differentiation on six different typologies of polyelectrolyte nanofilms is evaluated and quantified, giving a reference for skeletal muscle regeneration capabilities on such kind of structures.

³ Author to whom any correspondence should be addressed.

1. Introduction

Polyelectrolyte nanofilms are interesting structures generally obtained by layer-by-layer (LbL) method, consisting of consecutive adsorption of polyanions and polycations. Layer thickness and interlayer separation are controllable at the nanometer scale, thus allowing to obtain robust and homogeneous films with tunable thickness (Decher 1997). The importance of biocompatible materials made by LbL has been highlighted in many studies (Elbert *et al* 1999, Ngankam *et al* 2000, Katsuhiko *et al* 2006), and it can be mainly ascribed to the possibility to obtain conformal thin film coatings with precisely tuned physical, biochemical, and chemical properties. This aspect is of paramount importance to preserve normal cell activity and to maintain tissue-specific function on synthetic scaffolds. Poly(sodium-4-styrene sulfonate) (PSS) and poly(allylamine hydrochloride) (PAH) are two synthetic polymers, negatively and positively charged respectively, which have been already presented in literature as main component of multilayer polyelectrolyte nanofilms. These multilayer biocompatible structures showed a linear growth of both mass and film thickness with the number of deposited layers (Caruso *et al* 1997). Polymers in exponentially growing films can diffuse within the entire film structure and whether the terminal layer is cationic or anionic does not influence cell adhesion (Guillame-Gentil *et al* 2010). The situation is different for the polyelectrolyte multilayers used in the present study: such films have a stratified structure, and each polyelectrolyte layer interpenetrates only its neighbouring layers (Boudou *et al* 2010). The possibility to adjust chemical, physical, and mechanical properties of these kinds of synthetic polymers attracted much interest in relation to the influence of such parameters on adherent cell behaviour. Adhesion, proliferation and subsequent differentiation are the main events occurring when cells come into contact with a material surface (Ratner *et al* 1996, Rehfeldt *et al* 2007). In the case of synthetic polyelectrolytes such as PSS/PAH films, initial cell adhesion is mostly mediated through electrostatic interaction and, more indirectly, it is favoured by serum proteins absorption on the film surface (Ladam *et al* 2002, Salloum and Schlenoff 2004). PSS/PAH films have been tested with different cell lines, such as fibroblasts (Shim *et al* 2007), human hepatocellular carcinoma cells and human fetal hepatoblasts (Wittmer *et al* 2008), smooth muscle cells (Li *et al* 2005), umbilical vein endothelial cells (HUVECs) (Moby *et al* 2007), rabbit endothelial progenitor cells (EPCs) (Berthelemy *et al* 2008), human progenitor-derived endothelial cells (PDECs) (Thébaud *et al* 2010), and osteoblasts (Tryoen-Tóth *et al* 2001). Concerning skeletal muscle cells, C2C12 myoblasts have been cultured on different types of polyelectrolyte films, such as poly(L-lysine)/Hyaluronan (PLL/HA) (Ren *et al* 2008, Vázquez *et al* 2009), poly(acrylic acid)/poly(acryl amide) (PAA/PAAm) and poly(acrylic acid)/poly(allyl amine hydrochloride) (PAA/PAH) (Richert *et al* 2008); based on the authors' knowledge, the evaluation and quantification of growth and differentiation of C2C12

on PSS/PAH films have not been addressed up to now. C2C12 is a muscle-like cell line, capable of differentiation of myoblasts, thus forming contractile myotubes. The aim of the present study is to investigate how C2C12 cell activity can be modulated using PSS/PAH LbL nanofilms, varying some of the fabrication parameters. These synthetic structures are thought to be used as biomaterial coatings, and it is therefore important to know which is their effect (not necessarily a positive one) on different cell populations. This paper provides a quantitative reference for proliferation and differentiation capabilities of C2C12 cells on such kind of structures. Here we describe the preparation method to obtain PSS/PAH nanofilms made by 60, 80, 100, and 120 layers with a variable PSS molecular weight, thus obtaining thicknesses between 40 nm and 90 nm. We report the characterization of such nanofilms in terms of thickness and surface roughness, clarifying the choice of the 80 layers nanofilms as preferred substrate for cellular tests. We finally describe the behaviour of C2C12 cells cultured on them, quantifying the proliferation and differentiation capabilities of myoblasts onto 6 film typologies, differing for the polyelectrolyte used as top layer, and for the PSS molecular weight.

2. Materials and methods

2.1 Polyelectrolyte nanofilm preparation

Silicon wafers (Si-Mat Silicon Materials, Germany), used as substrates for film deposition, were cut in squares (2 cm x 2 cm), treated using an acid mixture (SPM: 96% H₂SO₄: 30% H₂O₂ = 4:1 (v/v)) at 120°C for 10 min, and then thoroughly rinsed with deionized water (d-H₂O). Different PSS, having distinct molecular weights (PSS1, M_w 76,000 Da; PSS2, M_w 200,000 Da; and PSS3, M_w 1,000,000 Da, Sigma Aldrich) and PAH (M_w 56,000 Da, Sigma Aldrich) were used as anionic and cationic polymers, respectively. In this study, all the polyelectrolyte aqueous solutions of PSS (0.5 wt.%) and PAH (0.5 wt.%) were used without pH adjustment and without addition of ionic salt. The SA-LbL deposition was carried out as follows: few drops of polyelectrolyte solution were placed on the silicon substrate, that was rotated with a spinner at 3000 rpm for 15 s. After the deposition of each polyelectrolyte layer, the substrates were thoroughly rinsed twice with d-H₂O and then dried by spinning for 15 s with a rotation speed of 4500 rpm. The polycation/polyanion deposition steps were repeated until the multilayer film was built and constituted by the desired number of layers and the desired polyelectrolyte as top layer. All the preparation routines for polymeric nanofilm fabrication were performed in a clean-room (class 1000) to avoid contamination. Different types of nanofilms were prepared changing the stacking sequence.

In the present paper, we use abbreviations for the different film typologies. PSS1, PSS2, and PSS3 stand for the three different PSS molecular weights used in the study (76,000, 200,000, and 1,000,000 Da, respectively). PSS1_n⁺ stands for (PAH-PSS1)_n-PAH, while PSS1_n⁻ stands for (PAH-PSS1)_n, corresponding to films constituted of *n* pairs of layers and with PAH or PSS1 as top layer, respectively. The same nomenclature is used for films constituted of PSS2 and PSS3.

2.2 Nanofilm characterization

Nanofilm morphology, thickness and surface roughness were evaluated by a Veeco Innova Scanning Probe Microscope (Veeco Instruments Inc., Santa Barbara, CA) operating in tapping mode, using a RTESPA Al coated silicon probe (Veeco Instruments Inc.), with an elastic modulus of 20-80 N/m, a resonance frequency of 235-317 kHz and an average tip radius of 8 nm. All the measurements were performed in air, at room temperature on SiO₂ supported nanofilms.

For thickness measurements, the sample was scratched with a needle and then scanned across the edge of the scratch over a 20 μm × 20 μm area, recording 64 × 64 samples. By elaborating the resulting scan data by software analysis (SPMLab software Version 5.01), we quantified the nanosheet thickness measuring the height profile of the edge. For roughness measurements, the surface was scanned in tapping mode over 20 μm × 20 μm and 5 μm × 5 μm areas, collecting 512 × 512 samples, and recording topography, phase and amplitude channels.

2.3 Cell culture and in vitro analysis

C2C12 mouse myoblasts (ATCC, CRL-1772) were expanded using a culture medium, constituted by Dulbecco's modified Eagle's medium (DMEM) supplemented with 10% fetal bovine serum (FBS), 100 IU/mL penicillin, 100 μg/mL streptomycin and 2 mM L-glutamine. Cells were maintained at 37°C, in a saturated humidity atmosphere (95% air / 5% CO₂). Differentiation of C2C12 myoblasts in myotubes was initially induced by switching, in cell specimens at ~90% confluence, the culture medium from expansion to differentiation medium, constituted by DMEM supplemented with 2mM glutamine, 100 IU/mL penicillin, 100 μg/mL streptomycin, 1% Insulin-Transferrin-Selenium ([ITS] I3146; Sigma, St. Louis, MO), and 1% FBS. To allow late differentiation, starting from the 3rd day of culture in differentiation medium, the samples were cultured in differentiation medium supplemented with 5 μg/mL AraC, which eliminates dividing cells. This kept the myoblasts from crowding out the myotubes, and allowed a myotube culture to be maintained for 1 week.

Before C2C12 seeding, nanofilms attached to a Si wafer (5 x 5 mm) were immersed in phosphate buffer saline (PBS) solution, supplemented with 2 mg/mL streptomycin for 30 min, in order to sterilize them, and subsequently rinsed three times with sterile PBS.

For qualitative vitality studies, 15,000 cells/cm² were seeded on the film surface and the sample cultured for 24 h in expansion medium. At the end of the 24 h, vitality of cells on the samples (3 samples for each typology) was investigated using the LIVE/DEAD[®] Viability/Cytotoxicity Kit (Molecular Probes, L3224). With such kit, live and dead cells can be identified on the basis of their membrane integrity and esterase activity. Briefly, after removing the culture medium, the samples were rinsed with PBS. 2 µM calcein AM and 4 µM EthD-1 in PBS were added, and incubation at 37°C for 10 min was performed. Samples were finally observed with an inverted fluorescent microscope (Eclipse Ti, FITC-TRITC filters, Nikon) equipped with a cooled CCD camera (DS-5MC USB2, Nikon) and with NIS Elements imaging software.

For proliferation studies, 15,000 cells/cm² were seeded on the film surface and the samples cultured for 72 h in expansion medium. At the end of the 72 h, double-stranded (ds)-DNA quantification on the samples (3 samples for each typology) was performed. Briefly, after removing the culture medium, double distilled water (dd)-H₂O was added to the samples. They were then immediately frozen at -20°C and stored for subsequent assays. The PicoGreen kit (Molecular Probes) was used in order to measure ds-DNA content in cell lysates. PicoGreen dye and working buffer solutions were prepared according to the manufacturer's instructions and 100 µL and 150 µL for each well added, respectively. Samples were incubated at room temperature for 10 min in the dark, and fluorescence intensity was then measured on a plate reader (Victor3; PerkinElmer, Waltham, MA) using an excitation wavelength of 485 nm and an emission wavelength of 535 nm.

For metabolic activity studies, 15,000 cells/cm² were seeded on the film surface and the samples cultured for 72 h in expansion medium. 90 min before the endpoint, WST-1 assays were carried out on the samples (3 samples for each typology). The culture medium was removed from the samples and 100 µL of culture medium + 10 µL of 2-(4-iodophenyl)-3-(4-nitrophenyl)-5-(2,4-disulfophenyl)-2H-tetrazolium monosodium salt, provided in a pre-mix electro-coupling solution (BioVision), were added. After 90 min of incubation at 37°C, absorbance at 450 nm was read with a microplate reader.

For differentiation studies, cells were seeded at confluence on the film surface. The samples were cultured in expansion medium for 24 h, after which the medium was switched towards differentiation medium. Samples were then cultured replacing the medium every day. At the required endpoints (3rd and 7th day of differentiation) the samples were treated for nucleus and F-actin staining, using a standard immunofluorescence protocol. 1 µM DAPI (Invitrogen) and 100 µM

Oregon Green[®] 488 phalloidin (Invitrogen) in PBS were used, and after 30 min incubation the samples were observed with the inverted fluorescent microscope.

The fusion index of the cultures was calculated, in order to quantitatively evaluate the differentiation grade of cells on the different samples. Such index was determined by dividing the total number of nuclei in myotubes (≥ 2 nuclei) by the total number of nuclei counted. The total myotube area, calculated as the percentage of the total image area covered by myotubes (Ren *et al* 2008), is another parameter that we used to evaluate cell differentiation. Experiments were performed on three samples for each film typology, and by analyzing 5 low magnification images for each sample.

Analysis of data was performed by analysis of variance (ANOVA) followed by Holm-Sidak tests in order to evaluate differences among groups. Significance was set at 5%.

3. Results and discussion

3.1 Nanofilm structure and characterization results

The six nanofilm typologies (PSS1_n⁺, PSS2_n⁺, PSS3_n⁺, PSS1_n⁻, PSS2_n⁻, PSS3_n⁻) were built varying the number of bilayers; thus morphology, film thickness and surface roughness were evaluated by means of AFM measurements. Figure 1 shows the results obtained.

Figure 1. Nanofilm thickness (a) and surface roughness (b) for the six nanofilm typologies. Thickness and roughness measurements were performed in triplicate for each film type. On the right, morphology of nanofilms with 40 couples is shown.

As expected, nanofilm thickness linearly increases with the number of bilayers (Caruso *et al* 1997). Statistically significant differences among different nanofilm typologies having the same number of layers were not evidenced. This indicates that the thickness increment per deposited pair of layers for PSS/PAH films is independent of the polyelectrolytes molecular weights. These results are in agreement with previous studies reporting the molecular weight independence of film growth curve and thickness of exponentially growing films (Porcel *et al* 2007). Nanofilm surface roughness increases with PSS molecular weight, but it does not significantly change with the terminal layer keeping the PSS molecular weight constant. A small - but statistically significant - difference in terms of surface roughness can be observed varying the number of bilayers, but the overall range is restrained between 4 and 12 nm. By performing AFM imaging after immersion of the nanofilm in culture medium for 24 h, a change in the nanofilm surface was evidenced (data not shown). The

film surface results covered by a uniform layer, changing the final height of the film and its roughness (the final roughness is about 4 nm less in comparison with the non-serum covered sample). No differences were remarkable among PAH-terminal and PSS-terminal serum covered samples having the same PSS molecular weight.

We chose the 40 bilayers samples as substrates for cellular tests, because of their nanometric thickness (57 ± 5 nm), surface roughness (7.5 ± 3.4 nm), and reasonable time needed for their fabrication (~ 90 min). As known, a higher level of roughness would be maybe preferable, in order to have a better cellular response in terms of adhesion and proliferation (Richert *et al* 2008, Ciofani *et al* 2010), but a compromise with the fabrication constraints is needed, in order to build coating layers with reasonable cost and time.

3.2 Cell vitality, proliferation and metabolism assessment

The results obtained for qualitative cell vitality assessment, together with the quantification of the proliferation capability of C2C12 on the different polyelectrolyte nanofilms and their metabolic activity after 72 h of culture on these surfaces are reported in figure 2.

Figure 2. a) Viability/cytotoxicity staining of C2C12 on the 6 nanofilm typologies having PAH as top layer (left) or PSS as top layer (right). Dead cells are stained in red, live cells are stained in green. Scale bar is 100 μ m; quantification of proliferating capability (b) and metabolic activity (c) of C2C12 cultured for 72 h on the 6 nanofilm tipologies and on standard polystyrene controls. Tests were performed in triplicate for each sample typology.

There is a defined difference of cellular response between PAH-terminal layer and PSS-terminal layer samples. PAH-terminal layer films show a higher percentage of dead cells, increasing with the the increase of PSS molecular weight, and a rounded-shape cell morphology, that suggests a weak adhesion of cells to the substrate. PSS-terminal layer films show a low percentage of dead cells, decreasing with the increase of PSS molecular weight, and a well-spread cell morphology, that suggests a good adhesion of cells to the substrate. These preliminary observations seem in contrast with many literature evidences, describing positively charged surfaces (like poly(L-lysine) and polyethyleneimine) as good substrates for cell adhesion and proliferation (Bledi *et al* 2000, Mingyu *et al* 2004). However, has been also demonstrated that PAH-terminal films have a cell-selective behavior, promoting the attachment and growth of neuronal cells, but inhibiting the adhesion of neonatal rat cardiac and skeletal muscle cells (Dhir 2009), and that PSS-terminal films generally promote the attachment of different cell types, which can be ascribed to the presence of sulfonate

groups (Boudou *et al* 2010). In the long run, it would be useful to deeper investigate cell adhesion mechanisms on these substrates by means of quantitative single-cell force microscopy experiments (Benoit *et al* 2000), as well as to evaluate discrete interactions in cell adhesion by means of single-molecule force spectroscopy measurements (Selhuber-Unkel *et al* 2010).

To quantify the proliferation capability of C2C12 on the different polyelectrolyte nanofilms and their metabolic activity after 72 h of culture on these surfaces, ds-DNA quantification by means of PicoGreen kit and WST-1 test were performed. The results are coherent and in agreement with the qualitative results obtained at 24 h of culture. Concerning DNA quantification, from Figure 2b it is clear that PSS1₄₀⁺ and PSS1₄₀⁻ samples show almost the same cell number, while in PSS2₄₀⁺ and PSS3₄₀⁺ samples it is significantly lower. PSS2₄₀⁻ samples show a much greater cell proliferation rate respect to PSS1₄₀⁺ and PSS1₄₀⁻ samples (more than three times), tendency that is even greater in PSS3₄₀⁻ samples, even if statistical analysis shows no significance between PSS2₄₀⁻ and PSS3₄₀⁻ samples (p=0.07). Similar considerations can be done for WST-1 results (Figure 1c).

3.3 Cell differentiation evaluation

Differentiation evaluation was performed staining C2C12 nuclei and F-actin on the nanofilms at two endpoints (3rd and 7th day of differentiation). From the fluorescence images acquired at low magnification, it was then possible to quantify the differentiation grade, calculating the fusion index and the total myotube area. Figure 3 reports the obtained fluorescence images, after 3 and 7 days of differentiation.

Figure 3. Nuclei and F-actin staining of C2C12 after 3 days of differentiation (left panel) and after 7 days of differentiation (right panel) on polystyrene (top image) and on the 6 nanofilm tipologies having PAH as top layer (left) or PSS as top layer (right). PSS molecular weight increases from the top to the bottom. Nuclei are stained in blue, F-actin is stained in green.

Scale bar is 100 μ m.

After 3 days of differentiation, we can note some differences in myotube formation and shape among the different samples, those with PSS as top layer being characterized by a higher level of differentiation respect to the samples having PAH as top layer. This difference is probably due to the surface charges, the influence of which is related not only to adhesion and proliferation, but also to the differentiation process. This is confirmed by the higher differentiation level in PSS1₄₀⁺ respect to PSS2₄₀⁺ and PSS3₄₀⁺ samples. PSS1₄₀⁺ samples, in fact, having a lower molecular weight, are probably more affected by a surface charges compenetration among the different layers,

resulting in a top layer with positive but also negative charges, that promote differentiation in a more efficient way than the PSS2₄₀⁺ and PSS3₄₀⁺ samples. Myotube formation is enhanced on PSS-terminal films, with an increasing myotube percentage in correspondence to an increasing PSS molecular weight. Myotube formation on polystyrene controls is comparable with that of PSS-terminal samples. Same considerations can be done after 7 days of differentiation. Figure 4 shows the quantitative data extracted from fluorescence images.

Figure 4. Bar graphs showing fusion index and total myotube area for C2C12 cultured on the 6 film typologies and on polystyrene control. a) and b) refer to data after 3 days of differentiation; c) and d) refer to data collected after 7 days of differentiation. Both parameters were obtained by means of software analysis on 5 low magnification images for each sample typology. Each experiment was performed in triplicate.

The fusion index is quite low for PSS1₄₀⁺ and almost zero for PSS2₄₀⁺ and PSS3₄₀⁺ samples, while it reaches higher values for PSS1₄₀⁻, PSS2₄₀⁻, PSS3₄₀⁻, and polystyrene control samples. There is not statistically significant difference among the three PSS-terminal substrates and polystyrene samples, whose fusion index is around 20% and around 30% after 3 days and 7 days of differentiation, respectively. Concerning the total myotube area, PSS1₄₀⁺ samples show low values, while for PSS2₄₀⁺ and PSS3₄₀⁺ the parameter is close to zero. PSS-terminal samples show higher values of this parameter, with a strong tendency to increase in correspondence to a higher PSS molecular weight. The total myotube area values for PSS1₄₀⁻, PSS2₄₀⁻, and PSS3₄₀⁻ samples are significantly different, while the values for polystyrene control samples are similar to those of PSS2₄₀⁻ samples. Interestingly, both fusion index and total myotube area are not continuously decreasing with the increase of the molecular weight on PAH-terminal substrates. The smallest values, in fact, are those related to PSS2₄₀⁺ samples, while PSS3₄₀⁺ samples show slightly greater values. This result appears, at first sight, in contradiction with proliferation results. After 7 days of differentiation, few cells are still adhered to the PSS2₄₀⁺ and PSS3₄₀⁺ film surfaces (figure 3), but the percentage of cells fused together and forming myotubes is greater on PSS3₄₀⁺ samples. This can be explained taking into account the different mechanical properties of the samples (due to the different polymer molecular weight), that concur to influence myotube development.

4. Conclusions

In order to evaluate the use of multilayer polyelectrolyte nanofilms as tunable coating of substrates for cell culture, PSS/PAH polyelectrolyte films with variable number of layers, of PSS molecular weight and terminal layer were fabricated and characterized. Proliferation and differentiation of C2C12 skeletal muscle cells were quantified on 6 nanofilm typologies. Results showed that cell mortality is favored on PAH-terminal layer samples, while cell proliferation is higher on nanofilms with final PSS layer. Both phenomena increase, corresponding to a larger PSS molecular weight. We also reported quantitative data regarding C2C12 differentiation on the different substrates. PSS-terminal layer samples show a higher differentiation grade, which varies, in terms of total myotube area, among the different PSS molecular weights. In conclusion, the present study gives quantitative reference values concerning skeletal muscle regeneration capability on PSS/PAH multilayer films, that can be used to precisely tune the characteristics of biomaterial coatings in order to have predictable cellular responses. The possibility to change many parameters influencing cell behaviour, suggests that the use of polyelectrolyte multilayer films allows a more precise tuning and a wider range of the coating characteristics, in comparison with conventional surface coatings or surface plasma treatments. To better understand and predict cell behaviour on such structures, future studies will focus on a deeper characterization of the nanofilm in culture conditions. AFM analyses in dry state would allow to understand how and how much the nanofilm structure changes after protein coating and cell culture, as well as RCM measurements (Picart *et al* 2004).

Acknowledgments

Authors gratefully thank Mr. Carlo Filippeschi for his kind support during the clean-room procedures, Marco Salerno and Andrea Desii, for their contribution to the characterization experiments.

FIGURE CAPTIONS

Figure 1 - Nanofilm thickness (a) and surface roughness (b) for the six nanofilm typologies. Thickness and roughness measurements were performed in triplicate for each film type. On the right, morphology of nanofilms with 40 couples is shown (scale bar is 500 nm). For each substrate type, an exemplary height profile is reported (corresponding to the red line in the AFM image).

Figure 2 - a) Viability/cytotoxicity staining of C2C12 on the 6 nanofilm typologies having PAH as top layer (left) or PSS as top layer (right). Dead cells are stained in red, live cells are stained in green. Scale bar is 100 μm ; quantification of proliferating capability (b) and metabolic activity (c) of C2C12 cultured for 72 h on the 6 nanofilm tipologies and on standard polystyrene controls. Tests were performed in triplicate for each sample typology.

Figure 3 – Nuclei and F-actin staining of C2C12 after 3 days of differentiation (left panel) and after 7 days of differentiation (right panel) on polystyrene (top image) and on the 6 nanofilm tipologies having PAH as top layer (left) or PSS as top layer (right). PSS molecular weight increases from the top to the bottom. Nuclei are stained in blue, F-actin is stained in green. Scale bar is 100 μm .

Figure 4 – Bar graphs showing fusion index and total myotube area for C2C12 cultured on the 6 film typologies and on polystyrene control. a) and b) refer to data after 3 days of differentiation; c) and d) refer to data collected after 7 days of differentiation. Both parameters were obtained by means of software analysis on 5 low magnification images for each sample typology. Each experiment was performed in triplicate.

References

- Benoit M, Gabriel D, Gerisch G, and Gaub E 2000 Discrete interactions in cell adhesion measured by single-molecule force spectroscopy *Nat. Cell Biol.* 2 313-17
- Berthelemy N, Kerdjoudj H, Gaucher C, Schaaf P, Stoltz J F, Lacolley P, Voegel J C, and Menu P 2008 Polyelectrolyte films boost progenitor cell differentiation into endothelium-like monolayers *Adv. Mat.* 20 2674-78
- Bledi Y, Domb A J, and Linial M 2000 Culturing neuronal cells on surfaces coated by a novel polyethyleneimine-based polymer *Br. Res. Prot.* 5 282-89
- Boudou T, Crouzier T, Ren K, Bin G, and Picart C 2010 Multiple functionalities of polyelectrolyte multilayer films: new biomedical applications *Adv. Mat.* 22 441-67
- Caruso F, Niikura K, Furlong D N, and Okahata Y 1997 Ultrathin multilayer polyelectrolyte films on gold: construction and thickness determination *Langmuir* 13 3422-26
- Ciofani G, Ricotti L, Menciasci A, and Mattoli V 2010 Preparation, characterization and *in vitro* testing of poly (lactic-co-glycolic) acid/barium titanate nanoparticle composites for enhanced cellular proliferation *Biomed. Microdev.* DOI 10.1007/s10544-010-9490-6
- Decher G 1997 Fuzzy nanoassemblies: toward layered polymeric multicomposites *Science* 277 1232-37
- Dhir V 2009 Application of polyelectrolyte multilayers for photolithographic patterning of diverse mammalian cell types in serum free medium *Biotechnol. Prog.* 25 594-603
- Elbert D L, Herbert C B, and Hubbell J A 1999 Thin polymer layers formed by polyelectrolyte multilayer techniques on biological surfaces *Langmuir* 15 5355-62
- Guillame-Gentil O, Semenov O, Roca A S, Groth T, Zahn R, Vörös J, and Zenobi-Wong M 2010 Engineering the extracellular environment: strategies for building 2D and 3D cellular structures *Adv. Mat.* 22 5443-62
- Katsuhiko A, Takashi N, and Tsuyoshi M 2006 Immobilization of biomaterials to nano-assembled films (self-assembled monolayers, Langmuir-Blodgett films, and layer-by-layer assemblies) and their related functions *J. Nanosci. Nanotech.* 6 2278-301
- Ladam G, Schaaf P, Decher G, Voegel J C, and Cuisinier F J G 2002 Protein adsorption onto auto-assembled polyelectrolyte films *Biomol. Eng.* 19 273-80
- Li M, Mills D K, Cui T, and McShane M J 2005 Cellular response to gelatin- and fibronectin-coated multilayer polyelectrolyte nanofilms *IEEE Trans. Nanobiosci.* 4 170-79

- Mingyu C, Kai G, Jiamou L, Yandao G, Nanming Z, and Xiufang Z 2004 Surface modification and characterization of chitosan film blended with poly(L-lysine) *Biomater. Appl.* 19 59-75
- Moby V, Boura C, Kerdjoudj H, Voegel J C, Marchal L, Dumas D, Schaaf P, Stoltz J F, and Menu P 2007 Poly(styrenesulfonate)/poly(allylamine) multilayers: a route to favor endothelial cell growth on expanded poly(tetrafluoroethylene) vascular grafts *Biomacromol.* 8 2156-60
- Ngankam N A, Lavallo P, Voegel J C, Szyk L, Decher G, Schaaf P, and Cuisinier J G 2000 Influence of polyelectrolyte multilayer films on calcium phosphate nucleation *J. Am. Chem. Soc.* 122 8998-9005
- Picart C, Sengupta K, Schilling J, Maurstad G, Ladam G, Bausch A R, and Sackmann E 2004 Microinterferometric study of the structure, interfacial potential, and viscoelastic properties of polyelectrolyte multilayer films on a planar substrate *J. Phys. Chem. B* 108 7196-205
- Porcel C, Lavallo P, Decher G, Senger B, Voegel J C, and Schaaf P 2007 Influence of the polyelectrolyte molecular weight on exponentially growing multilayer films in the linear regime *Langmuir* 23 1898-904
- Ratner B D, Hoffman A S, Schoen F J, and Lemons J E 1996 *Biomaterials Science: An introduction to materials in Medicine*, Academic Press San Diego CA
- Rehfeldt F, Engler A J, Eckardt A, Ahmed F, and Discher D E 2007 Cell responses to the mechanochemical microenvironment – Implications for regenerative medicine and drug delivery *Adv. Drug. Deliv. Rev.* 59 1329-39
- Ren K, Crouzier T, Roy C, and Picart C 2008 Polyelectrolyte multilayer films of controlled stiffness modulate myoblast cells differentiation *Adv. Funct. Mater.* 18 1378-89
- Richert L, Vetrone F, Yi J H, Zalzal S F, Wuest J D, Rosei F, and Nanci A 2008 Surface nanopatterning to control cell growth *Adv. Mat.* 20 1488-92
- Salloum D S, and Schlenoff J B 2004 Protein adsorption modalities on polyelectrolyte multilayers *Biomacromolecules* 5 1089-96
- Selhuber-Unkel C, Erdmann T, López-García M, Kessler H, Schwarz U S, and Spatz J P 2010 Cell adhesion strength is controlled by intermolecular spacing of adhesion receptors *Biophys. J.* 98 543-51
- Shim H W, Lee J H, Hwang T S, Rhee Y W, Bae Y M, Choi J S, Han J, and Lee C S 2007 Patterning of proteins and cells on functionalized surfaces prepared by polyelectrolyte multilayers and micromolding in capillaries *Biosens. Bioelectr.* 22 3188-95
- Thébaud N B, Bareille R, Daculsi R, Bourget C, Rémy M, Kerdjoudj H, Menu P, and Bordenave L 2010 Polyelectrolyte multilayer films allow seeded human progenitor-derived endothelial cells to remain functional under shear stress in vitro *Acta Biomater.* 6 1437-45

- Tryoen-Tóth P, Vautier D, Haikel Y, Voegel J C, Schaaf P, Chluba J, and Ogier J 2001 Viability, adhesion, and bone phenotype of osteoblast-like cells on polyelectrolyte multilayer films *J. Biomed. Mat. Res.* 60 657-67
- Vázquez C P, Boudou T, Dulong V, Nicolas C, Picart C, and Glinel K 2009 Variation of polyelectrolyte film stiffness by photo-cross-linking: a new way to control cell adhesion *Langmuir* 25 3556-63
- Wittmer C R, Phelps J A, Lepus C M, Saltzman W M, Harding M J, and Van Tassel P R 2008 Multilayer nanofilms as substrates for hepatocellular applications *Biomaterials* 29 4082-90

Figure 1

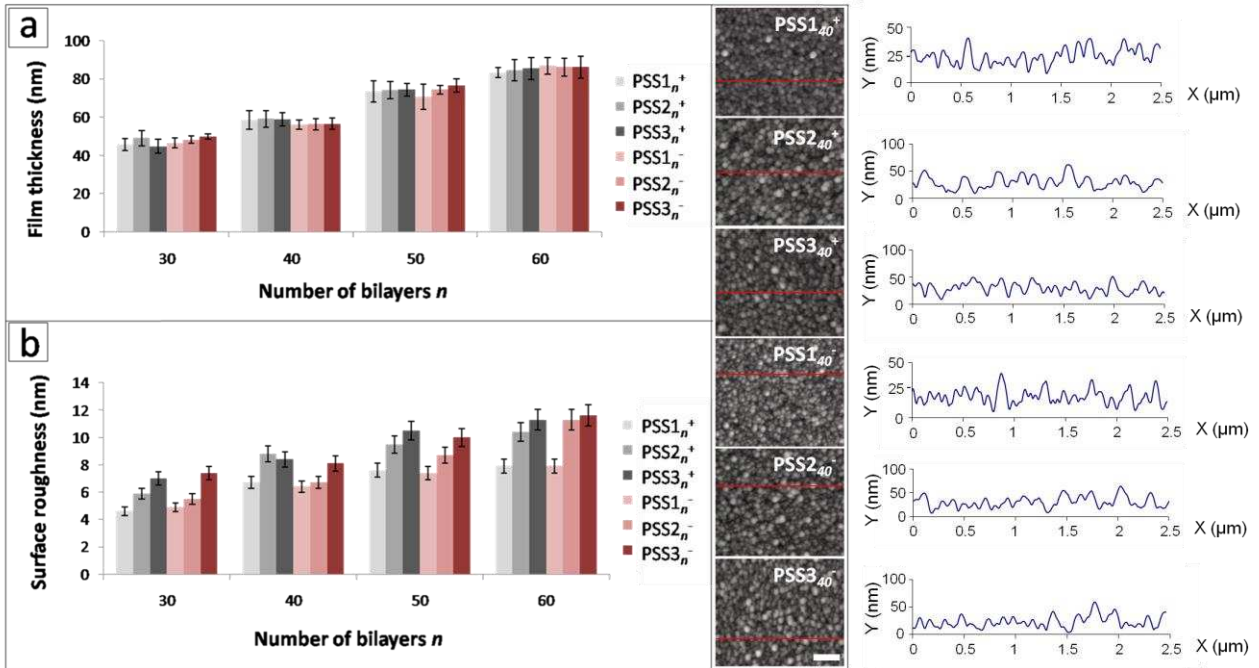


Figure 2

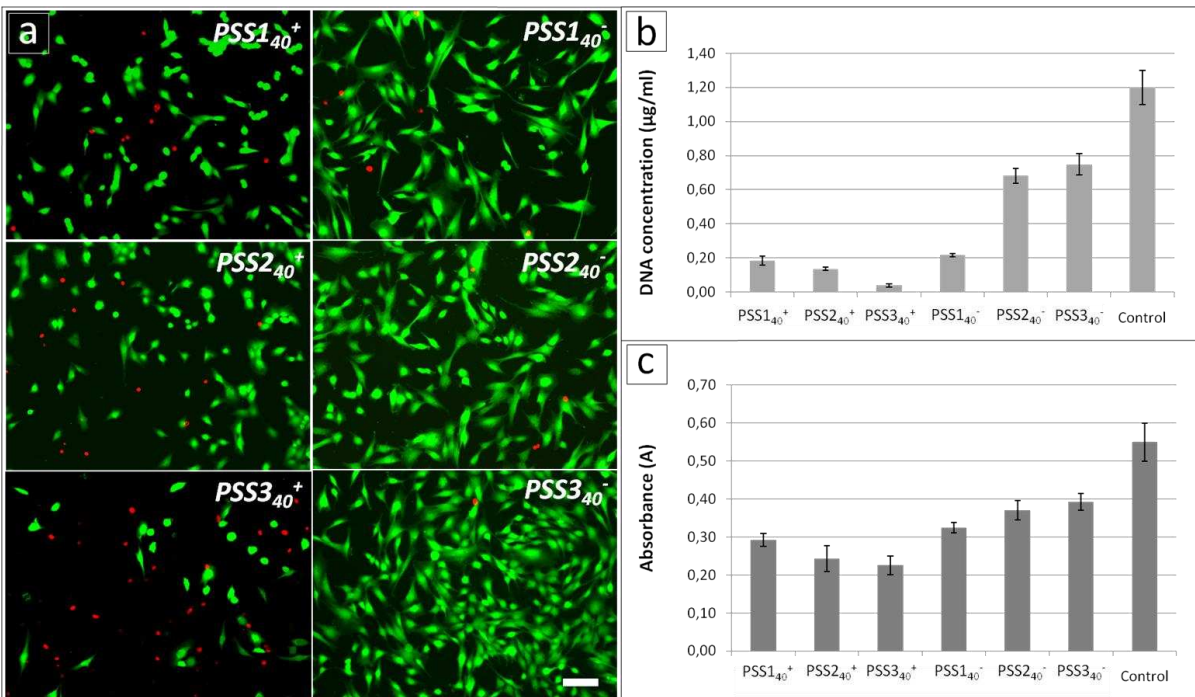


Figure 3

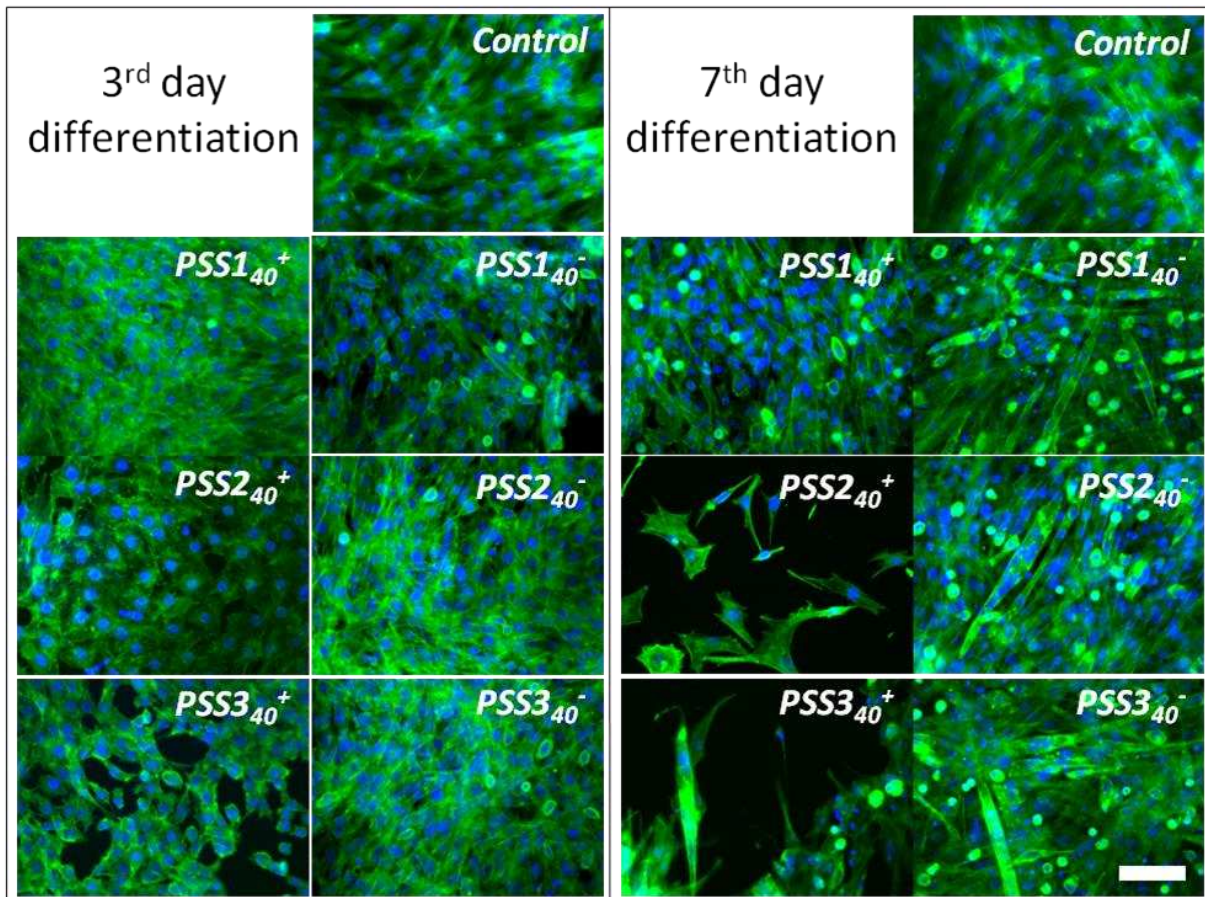


Figure 4

